

# Ranking the Brønsted Acid Strength of Protonic Zeolites with VTIR Spectroscopy — An Overview of Current Research

© C.O. Arean, M.R. Delgado<sup>¶</sup>

Department of Chemistry, University of the Balearic Islands, 07122 Palma, SPAIN

<sup>¶</sup>e-mail: montserrat.rodriquez@uib.es

Received March 05, 2022

Revised March 05, 2022

Accepted March 11, 2022

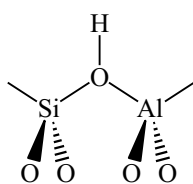
Many industrial applications of protonic zeolites as solid-acid heterogeneous catalysts rely on the strength of their Brønsted acidity, which (together with zeolite topology) affects both, catalytic activity and selectivity. Therefore, the convenience to have an accurate (and simple) experimental technique for measuring Brønsted acid strength. The enthalpy change,  $\Delta H^0$ , corresponding to the hydrogen bonding interaction of a weak base (such as CO or dinitrogen) with their Brønsted acid [Si(OH)Al] hydroxyl groups should directly correlate with the zeolite acid strength. Nevertheless, because of simplicity, the bathochromic shift of the O–H stretching frequency,  $\Delta\nu_{(\text{OH})}$ , is usually measured by IR spectroscopy at a low temperature, and correlated with acid strength, for ranking zeolite acidity. Herein the use of variable-temperature IR (VTIR) spectroscopy to determine simultaneously  $\Delta H^0$  and  $\Delta\nu_{(\text{OH})}$  is demonstrated; followed by an abridged overview showing that direct correlation between  $\Delta\nu_{(\text{OH})}$  and Brønsted acid strength can be misleading when ranking zeolite acidity.

**Keywords:** VTIR spectroscopy, Brønsted acidity, H-zeolites

DOI: 10.21883/EOS.2022.05.54433.17-22

## 1. Introduction

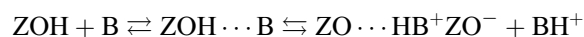
By virtue of their [Si(OH)Al] units (see below) protonic zeolites show a distinctive Brønsted acidity which endows them with widespread application as solid acid catalysts in a wide range of chemical processes spanning the fields of selective reforming of hydrocarbons, methanol to olefin conversion, biomass upgrading and the manufacture of fine chemicals, to quote only a few examples [1–5].

**Scheme 1.** Sketch of a zeolite Brønsted acid site.

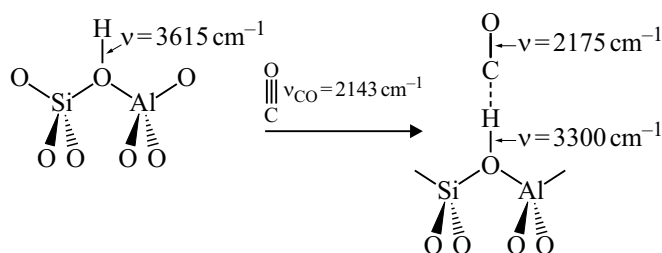
Taken together with zeolite topology and Si:Al ratio, the strength of their (catalytically active) Brønsted acid sites is a major factor determining the catalytic performance of protonic zeolites in terms of both, catalytic activity and selectivity; and therefore, the convenience to have a reliable method to quantify the relative Brønsted acidity of protonic zeolites [6,7]. To that purpose both, IR and solid-state NMR spectroscopy stand out from the repertoire of instrumental techniques most frequently used; and the same applies when it comes to explore the surface chemistry of both, zeolites and microporous aluminosilicates in a broader context [8–17]. IR spectroscopy will be dealt with herein.

Classical IR spectroscopy (at liquid nitrogen temperature) of an adsorbed weak base, such as carbon monoxide,

is very often the technique of choice for determining zeolite Brønsted acidity: but dinitrogen could also be used, instead of CO. In principle, proton transfer from the zeolite Brønsted acid site (ZOH) to a sufficiently strong base (B) would involve both; hydrogen-bonded and ion-pair intermediate species, as shown below:



Nevertheless, in the case of a weak base the process stops before the detached ion pair is formed; and that is the case for carbon monoxide, as shown in Scheme 2:

**Scheme 2.** Wavenumbers are illustrative; actual values depend on the specific zeolite being considered.

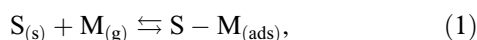
Formation of the hydrogen-bonded  $\text{ZOH} \cdots \text{CO}$  complex brings about a large bathochromic shift,  $\Delta\nu_{(\text{OH})}$ , of the corresponding O–H stretching mode which is easily measured by IR spectroscopy; and the magnitude of that wavenumber shift is usually assumed to correlate directly with the Brønsted acid strength of the zeolite under study. This assumption, however, is not free from a number of possible pitfalls, as pointed out time ago by several

authors [14–17]. Moreover, some more recently reported results [18,19] showed a surprising difference between the apparent Brønsted acidity of some zeolites as determined from (i) the corresponding  $\Delta\nu_{(\text{OH})}$  value, and (ii) the enthalpy change ( $\Delta H^0$ ) in the formation of the  $\text{ZOH} \cdots \text{CO}$  adsorption complex, as measured by variable-temperature IR (VTIR) spectroscopy.

## 2. Outline of the VTIR method

### 2.1. Bases

The VTIR method is an instrumental technique that enables one to gain access to gas-solid physisorption thermodynamics while simultaneously obtaining the IR spectroscopic signature of the gas adsorption complex, provided that either the solid adsorbent or the molecule being adsorbed from the gas phase has an IR active mode which undergoes a change in the adsorption process. That being the case, let Eq. (1) represent the adsorption equilibrium:



where S stands for the adsorption site and M for the adsorbed molecule. Should the adsorption process follow the Langmuir model, the characteristic wavenumber of the IR absorption band under study would not change along the series of IR spectra obtained, while the corresponding integrated absorbance would be proportional to surface coverage,  $\theta$ , (Lambert Beer law) thus giving the activity (in the thermodynamic sense) of both, the adsorbed species and the empty sites,  $(1 - \theta)$ , while the activity of the gas phase is given by the corresponding equilibrium pressure,  $p$ . Thereby, measurement of IR absorbance and equilibrium pressure at any given temperature ( $T$ ) leads to the value of the equilibrium constant,  $K$ , for Eq. (1) at that temperature. Assuming that changes in specific heat are negligible [20] the variation of  $K$  with temperature,  $T$ , should be related to the standard adsorption enthalpy,  $\Delta H^0$ , and entropy,  $\Delta S^0$ , by the van't Hoff equation:

$$K(T) = \exp[-\Delta H^0/RT] p \exp[\Delta S^0/R]. \quad (2)$$

Combination of Eq. (2) with the Langmuir Eq. (3) leads to Eq. (4) below:

$$\theta = K(T)p/[1 + K(T)p] \quad (3)$$

$$\ln[\theta/[(1 - \theta)p]] = (-\Delta H^0/RT) + (\Delta S^0/R) \quad (4)$$

which can also be written as:

$$\ln[A/[(A_M - A)p]] = (-\Delta H^0/RT) + (\Delta S^0/R) \quad (5)$$

where  $A$  stands for the actual IR absorbance being measured, and  $A_M$  is the maximum absorbance, which corresponds to  $\theta = 1$ .

It should thus be clear that after determining  $\theta$  (or relative IR absorbance) as a function of  $T$  and  $p$  over a temperature

range, equations (4) or (5) give direct access to the values of  $\Delta H^0$  and  $\Delta S^0$  that characterize the gas adsorption process. Worth of notice is that series of VTIR spectra should always be recorded over a sufficiently wide temperature range; otherwise spurious correlations between  $\Delta H^0$  and  $\Delta S^0$  can occur [21,22].

### 2.2. Experimental protocol

A properly designed IR cell is needed for recording VTIR spectra. Some commercial cells can be adapted for such a purpose, but the experimental results reviewed herein were obtained using a homemade cell described in detail elsewhere [23], which was equipped with a platinum resistance thermometer (Tinsley) inserted close to the sample wafer and a capacitance pressure gauge (MKS, Baratron). The precision of the corresponding measurements was  $\pm 10^{-2}$  mbar and  $\pm 2$  K for pressure and temperature, respectively. The protocol for recording VTIR spectra is described below, with specific reference to H-FER.

## 3. Selected cases reviewed

### 3.1. H-FER zeolite probed with CO

A sample of H-FER, having a nominal Si:Al ratio of 27.5:1, was obtained from a commercial firm and checked by powder X-ray diffraction, which showed good crystallinity and absence of diffraction lines not assignable to the corresponding structure type. For VTIR spectroscopy a thin self-supported wafer of the zeolite was prepared and activated (outgassed) by thermal treatment in a dynamic vacuum (residual pressure  $< 10^{-4}$  mbar) inside the IR cell, which was then cooled with liquid nitrogen. After recording the zeolite blank spectrum, the cell was dosed with just the right amount of CO to form a 1:1 adsorption complex on every Brønsted-acid (OH group) of the zeolite. Having done that, the cell was closed and series of FTIR spectra were registered upon gradual warming up. To avoid repetition, please keep in mind that (basically) the same protocol was applied to obtain VTIR spectra of each protonic zeolite reviewed herein.

The application of VTIR spectroscopy to the study of carbon monoxide in a sample of H-FER was reported in detail elsewhere [24]. For the purpose of this overview, Figure 1 displays a set of representative spectra in the O–H stretching region. Figure 1, *a* reports the zeolite blank spectrum and also after dosing with CO at 77 K. The zeolite blank spectrum shows characteristic IR absorption bands peaking at 3747 and at 3605  $\text{cm}^{-1}$ , which should be assigned, respectively, to silanols and to the bridged  $[\text{Si}(\text{OH})\text{Al}]$  hydroxyl groups that constitute the zeolite Brønsted-acid sites [8]. Dosing with CO (in the low-pressure range studied herein) did not significantly alter the silanols band, whereas the intensity of the 3605  $\text{cm}^{-1}$  band decreased till an extent which was a function of temperature.

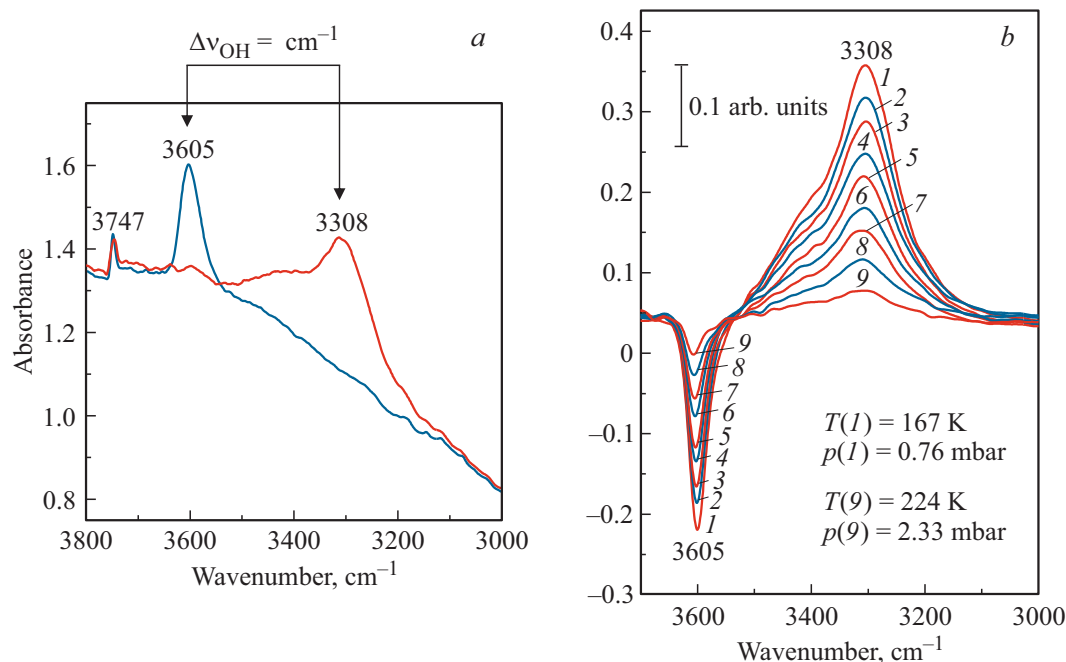


**Figure 1.** (a) IR spectra in the O–H stretching region of the zeolite blank wafer (blue line) and after dosing with CO at 77 K (red line). (b) Representative variable-temperature IR spectra (O–H stretching region) of CO adsorbed on H-FER. The spectra are shown in the difference mode (zeolite blank subtracted). From 1 to 9, temperature goes from 167 to 224 K; and equilibrium pressure from 0.76 to 2.33 mbar.

Simultaneously, a much broader band appears showing a maximum at around 3308 cm<sup>−1</sup>, which corresponds to hydrogen-bonded OH⋯CO species ( $\Delta\nu_{\text{OH}} = 297 \text{ cm}^{-1}$ ). This is shown in Figure 1, b, which depicts some representative VTIR spectra in the difference mode; i.e., after subtracting the zeolite blank spectrum.

From 2 independent series of VTIR spectra, the van't Hoff linear plot shown in Figure 2 was obtained (square and circle points). Note that the integrated intensity of the 3605 cm<sup>−1</sup> band divided by its maximum value (i.e., that one corresponding to the zeolite blank spectrum) gives directly the fraction (1 −  $\theta$ ) of free OH sites, from which the corresponding  $\theta$  value needed for using the VTIR equation was obtained. This linear plot rendered the value of  $\Delta H^0 = -28.4 \text{ kJ mol}^{-1}$  for the standard enthalpy of formation of the OH⋯CO complex between the probe molecule and the Brønsted acid sites of H-FER. The estimated limit of experimental error is  $\pm 1 \text{ kJ mol}^{-1}$ . It's relevant to add that periodic DFT calculations [24] gave for the most stable OH⋯CO complexes  $\Delta H^0$  values in the range of  $-26$  to  $-29 \text{ kJ mol}^{-1}$ , in excellent agreement with the experimentally determined value of  $-28.4 \text{ kJ mol}^{-1}$ .

### 3.2. H-Ferrierite (H-FER) and N<sub>2</sub> as probe molecule

Selected VTIR difference spectra of dinitrogen adsorbed on H-FER are given in Figure 3, a, which shows that the Brønsted acid [Si(OH)Al] band at 3605 cm<sup>−1</sup> is increasingly

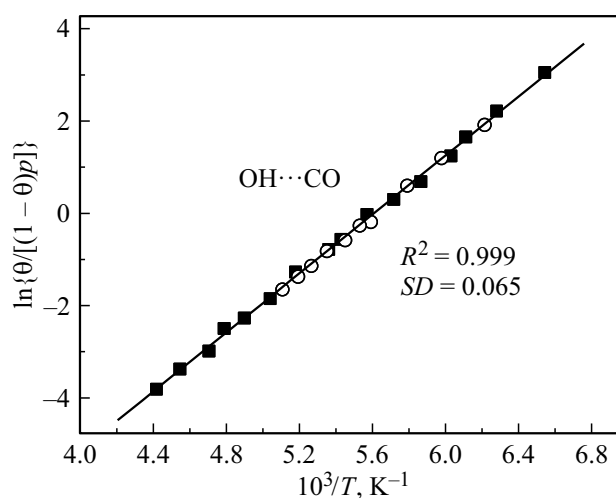


**Figure 2.** Van't Hoff plot for CO adsorbed on H-FER; data obtained from the O.H stretching band at 3605 cm<sup>−1</sup>. Data obtained from two independent series of IR spectra (squares and circles). R, linear regression coefficient; SD, standard deviation.

eroded when temperature decreases and simultaneously a new (broader) band centred at 3495 cm<sup>−1</sup> appears ( $\Delta\nu_{\text{OH}} = 110 \text{ cm}^{-1}$ ); as expected for the formation of hydrogen bonded OH⋯N<sub>2</sub> species with the zeolite Brønsted acid OH groups. From the whole set of data derived from two independent sets of VTIR measurements the van't Hoff plot shown in Figure 3, b was obtained (squares

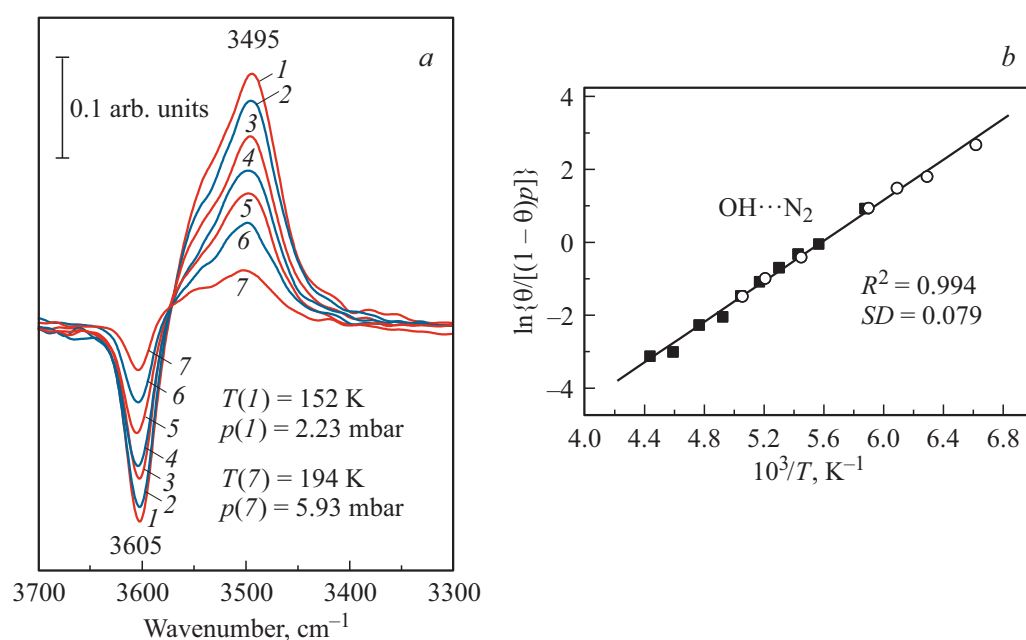


**Figure 3.** (a) Difference variable-temperature IR spectra (zeolite blank subtracted) of N<sub>2</sub> adsorbed on H-FER. The spectra are shown in the difference mode (zeolite blank subtracted). From 1 to 7, temperature goes from 152 to 194 K; and equilibrium pressure from 2.23 to 5.93 mbar. (b) Van't Hoff plot for N<sub>2</sub> adsorbed on H-FER; data obtained from the O–H stretching band at 3605 cm<sup>−1</sup> in two independent series of IR spectra (squares and circles). *R*, linear regression coefficient; SD, standard deviation.

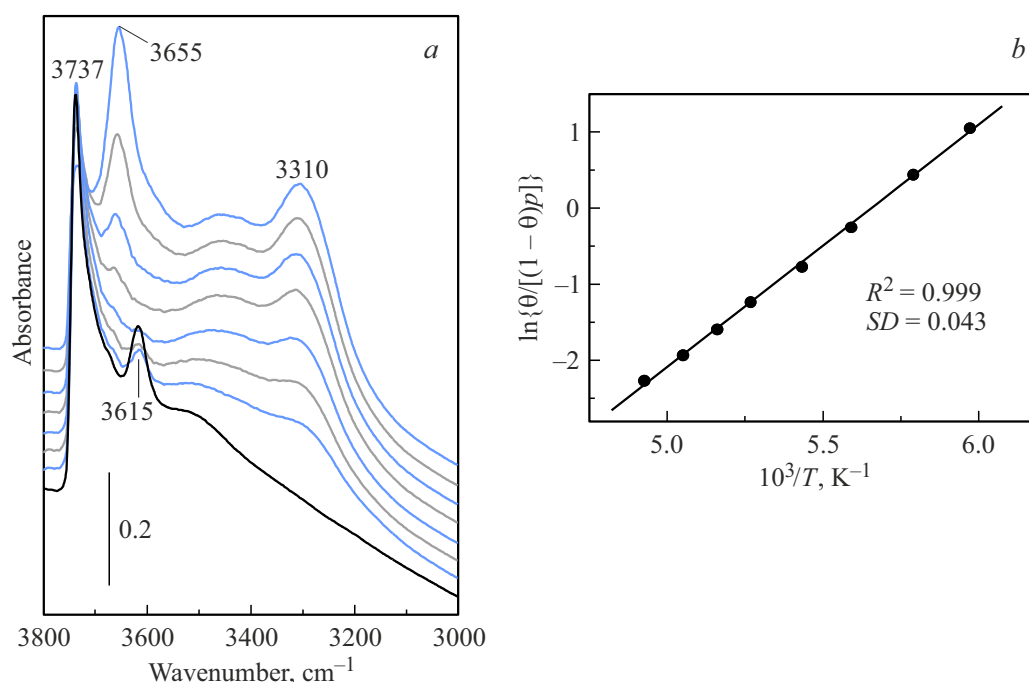


**Figure 4.** (a) Representative variable temperature IR spectra in the O–H stretching region of CO adsorbed on H-Beta. Blank zeolite spectrum shown in black. From top to bottom, temperature goes from 142 to 203 K, and equilibrium pressure from 4.69 to 10.59 mbar. (b) Van't Hoff plot for CO adsorbed on H-Beta; data obtained from the O–H stretching band at 3615 cm<sup>−1</sup>.

and circles). From the excellent linear fit obtained, the value of  $\Delta H^0 = -19.1 \text{ kJ mol}^{-1}$  for the standard adsorption enthalpy was derived; i.e., for hydrogen bonding between N<sub>2</sub> and the H-FER Brønsted acid sites. The estimated

error limit is  $\pm 1 \text{ kJ mol}^{-1}$ . It is relevant to add that the calculated values of  $\Delta H^0$  for the most stable OH...N<sub>2</sub> complexes were in the range of  $-17$  to  $-19 \text{ kJ mol}^{-1}$  [24], to be compared with the experimentally determined value

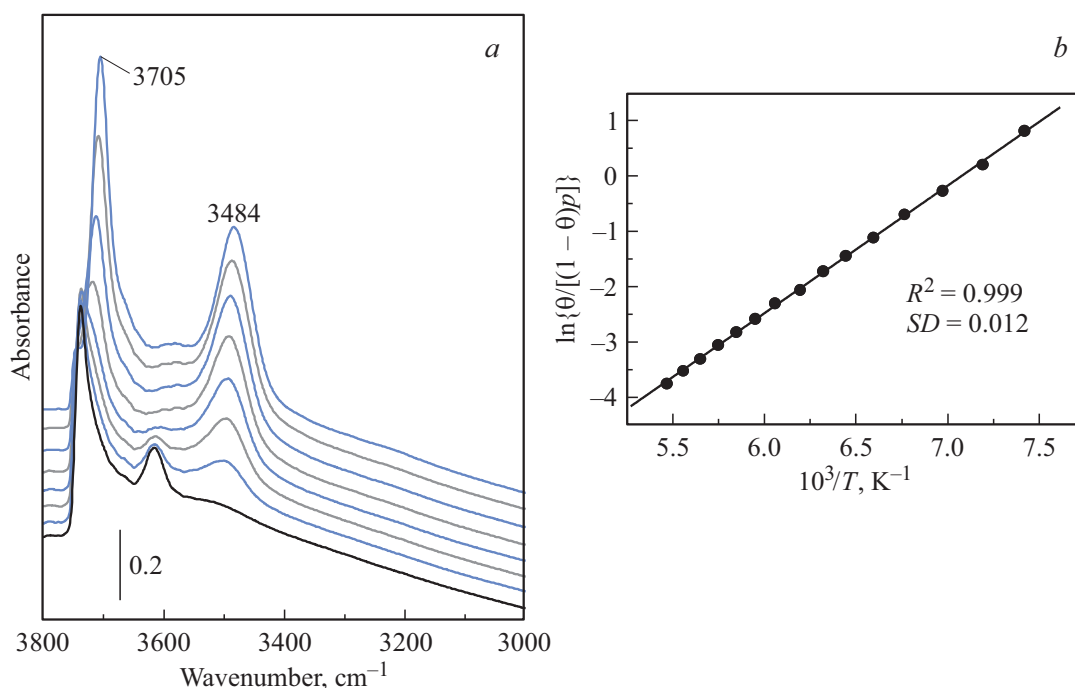


**Figure 5.** (a) Representative variable temperature IR spectra in the O–H stretching region of N<sub>2</sub> adsorbed on H-Beta. Blank zeolite spectrum shown in black. From top to bottom, temperature goes from 78 to 177 K, and equilibrium pressure from 0.13 to 11.58 mbar. (b) Van't Hoff plot for N<sub>2</sub> adsorbed on H-Beta; data obtained from the O–H stretching band at 3615 cm<sup>-1</sup>.

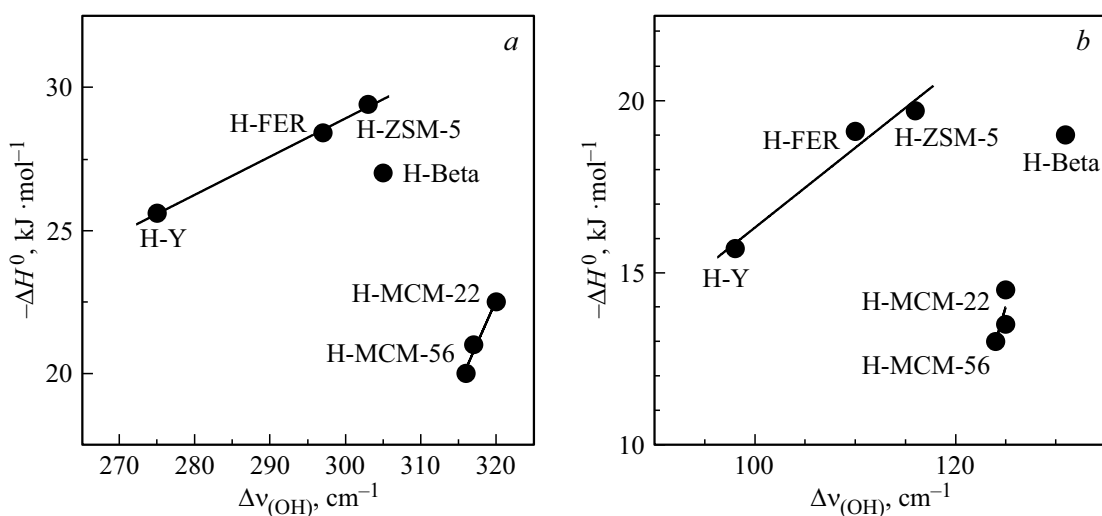


**Figure 6.** Correlation between  $\Delta H^0$  and  $\Delta\nu_{(OH)}$  for (a) CO and (b) N<sub>2</sub> hydrogen bonding in protonic zeolites.

of  $-19.1 kJ mol^{-1}$ . Again, there is a good agreement between calculated and experimentally determined standard enthalpy of formation of the hydrogen-bonded  $OH \cdots N_2$  species. Comparisons between  $\Delta H^0$  values obtained for  $OH \cdots CO$  and  $OH \cdots N_2$  complexes shows that the dinitrogen hydrogen-bonded complex is about  $10 kJ mol^{-1}$  less stable than the corresponding  $OH \cdots CO$  complex. A similar stability difference was found for other protonic zeolites, as shown below.

### 3.3. H-BETA and CO as probe molecule

The zeolite H-Beta considered herein was characterized in detail as described elsewhere [25]. Selected VTIR spectra for CO adsorbed on H-Beta are shown in Figure 4, a. The blank zeolite spectrum shows main IR bands at  $3737 cm^{-1}$  which is assigned to silanols and  $3615 cm^{-1}$  which corresponds to the zeolite Brønsted acid sites. After CO adsorption the  $3615 cm^{-1}$  band loses intensity to an extent that (as expected) is a function of temperature and

Relevant experimental data for CO and N<sub>2</sub> hydrogen bonding in protonic zeolites

Adsorbed probe molecule	Zeolite	Structure type	Si/Al ratio	$\Delta\nu_{(\text{OH})}^a$ cm <sup>-1</sup>	$-\Delta H^b$	Ref.
CO	H-Beta	BEA	20	305	27	[25]
	H-ZSM-5	MFI	30	303	29.4	[26]
	H-FER	FER	27.5	297	28.4	[24]
	H-Y	FAU	5.6	275	25.6	[27]
	H-MCM-22	MWW	24.5	320	22.5	[19,28]
	H-MCM-22	MWW	16.4	317	21	[19]
	H-MCM-56	MWW	16	316	20	[19]
	H-MCM-56	MWW	16	124	13	[19]
N <sub>2</sub>	H-Beta	BEA	20	131	19	[25]
	H-ZSM-5	MFI	30	116	19.7	[20,26]
	H-FER	FER	27.5	110	19.1	[24]
	H-Y	FAU	5.6	98	15.7	[26]
	H-MCM-22	MWW	24.5	125	14.5	[19,28]
	H-MCM-22	MWW	16.4	125	13.5	[19]
	H-MCM-56	MWW	16	124	13	[19]
	H-MCM-56	MWW	16	124	13	[19]

Note. <sup>a</sup> Red-shift of the Brønsted-acid OH group upon hydrogen bonding with CO or N<sub>2</sub>. <sup>b</sup> Standard enthalpy change in the formation of the OH...M complex (M = CO, N<sub>2</sub>).

equilibrium pressure. Simultaneously, a new IR absorption band builds up at 3310 cm<sup>-1</sup>;  $\Delta\nu_{(\text{OH})} = 305$  cm<sup>-1</sup> (note also that the silanol band at 3737 cm<sup>-1</sup> is also partially eroded and gives rise a well-defined absorption band at 3655 cm<sup>-1</sup>). From the whole set of VTIR spectra obtained, the van't Hoff plot shown in Figure 4, *b* was obtained, which gave the value of  $\Delta H^0 = -27(\pm 1)$  kJ mol<sup>-1</sup> for the standard adsorption enthalpy of CO adsorbed on the H-Beta Brønsted acid sites [25].

### 3.4. H-BETA and N<sub>2</sub> as probe molecule

Representative VTIR spectra of dinitrogen adsorbed on H-Beta are depicted in Figure 5, *a*, showing that, as in the case of CO, both the silanol band at 3737 cm<sup>-1</sup> and the Brønsted acid sites band at 3615 cm<sup>-1</sup> are affected by adsorption of the probe molecule; and simultaneously new IR absorption bands appeared at 3705 and 3484 cm<sup>-1</sup>, which testify to formation of the corresponding dinitrogen adsorption complexes. From the integrated intensity (obtained after background subtraction) the van't Hoff plot shown in Figure 5, *b* was obtained, which rendered the value of  $\Delta H^0 = -19(\pm 1)$  kJ mol<sup>-1</sup> for the interaction between adsorbed dinitrogen and Brønsted acid OH groups [25].

## 4. Discussion and conclusions

In order to discuss the above results in a broader context, Table 1 summarizes relevant data reported in the literature for carbon monoxide and dinitrogen adsorption on several other protonic zeolites: H-ZSM-5 [20,26], H-Y [26,27], H-MCM-22 [19,28] and H-MCM-56 [19].  $\Delta H^0$  values involved in the formation of CO and N<sub>2</sub> hydrogen-bonded species were determined, in all cases, by means of VTIR spectroscopy. The derived correlation between  $\Delta H^0$  and  $\Delta\nu_{(\text{OH})}$  is depicted in Figure 6.

Inspection of this Table and Fig. 6, *a* show that the zeolites H-Beta, H-Y, H-FER and H-ZSM-5 display the expected trend for carbon monoxide, in the sense that increasing (absolute) values of  $\Delta\nu_{(\text{OH})}(\text{CO})$  correlate with increasing (absolute) values of  $\Delta H^0(\text{CO})$ , and the same trend applies to dinitrogen (Fig. 6, *b*); it is also worth of note that regardless of zeolite structure type and Si:Al ratio, the enthalpy of formation of the hydrogen-bonded OH...CO species is about 10 kJ mol<sup>-1</sup> greater (in absolute value) than the enthalpy of formation of the corresponding OH...N<sub>2</sub> species. Nevertheless, the most remarkable fact to consider is that the zeolites H-MCM-22 and H-MCM-56 (both with the same MWW structure type) break the rule correlating  $\Delta\nu_{(\text{OH})}$  with  $\Delta H^0$  for both, carbon monoxide and dinitrogen probe molecules. In fact, these zeolites show larger  $\Delta\nu_{(\text{OH})}$  values than the other protonic zeolites, and yet the corresponding  $-\Delta H^0$  values are smaller.

This observation should alert to the risk of using  $\Delta\nu_{(\text{OH})}$  values (after interaction of a protonic zeolite with CO or N<sub>2</sub>) as a measure of relative Brønsted acid strength; as shown herein, this practice can be misleading (at least in some cases). Determination of the corresponding interaction energy between the probe molecule and the Brønsted acid sites seems to be a more reliable test. For that purpose, VTIR spectroscopy can profitably be used, but other means are also available, both experimental and computational.

## References

- [1] J. Weitkamp. Zeolites and Catalysis, Solid State Ionics, **131**, 179 (2000).
- [2] S.H. Brown. Zeolites in Catalysis, Handbook of Green Chemistry. Ed. by Paul T. Anastas; Vol. 2: Heterogeneous Catalysis. (Wiley-VCH, Weinheim, 2009).
- [3] E.G. Derouane, H. He, S.B. Derouane-Abd Hamid, and I.I. Ivanova. Catal. Lett. **58**, 1 (1999).

- [4] M. Shamzhy, M. Opasenkov, P. Concepción, and A. Martinez. *Chem. Soc. Rev.* **48**, 1095 (2019).
- [5] N.V. Vlasenko, Y.N. Kochkin, G.M. Telbiz, O.V. Shvets, and P.E. Strizhak, *RSC Adv.* **9**, 35957 (2019).
- [6] C.O. Areal, *Ukr. J. Phys.* **63** (6) 538 (2018).
- [7] P. Losch, H.R. Joshi, O. Vozniuk, A. Grünert, C. Ochoa-Fernandez, H. Jabraoui, M. Badawi, and W. Schmidt, *J. Am. Chem. Soc.* **140**, 17790 (2018).
- [8] A. Zecchina, and C.O. Areal, *Chem. Soc. Rev.* **25** (3) 187 (1996).
- [9] A. Zheng, S. Li, S.-B. Liu, and P. Deng. *Acc. Chem. Res.* **49**, 655 (2016).
- [10] C.O. Areal, O.V. Manoilova, M.R. Delgado, A.A. Tsyganenko, and E. Garrone, *Phys. Chem. Chem. Phys.* **3**, 4187 (2001).
- [11] C.O. Areal, A.A. Tsyganenko, O.V. Manoilova, G.T. Palomino, M.P. Mentrui, and E. Garrone. *Chem. Commun.* **5**, 455 (2001).
- [12] C.O. Areal, A.A. Tsyganenko, E.E. Platero, E. Garrone, and A. Zecchina, *Angew. Chem. Int. Ed.* **37**, 3161 (1998).
- [13] H. Hadjiivanov, *Adv. Catal.* **57**, 99 (2014).
- [14] K.P. Schröder, J. Sauer, M. Leslie, C.R.A. Catlow, and J.M. Thomas. *Chem. Phys. Lett.* **188**, 320 (1992).
- [15] L.M.N. Barbosa, R.A. van Santen, and H. Hafner. *J. Am. Chem. Soc.* **123**, 4530 (2001).
- [16] L. Yang, K. Trafford, O. Kresnawahjuesa, J. Sepa, and R.J. Gorte. *J. Phys. Chem. B*, **105**, 1935 (2001).
- [17] K. Chakarova, and K. Hadjiivanov. *Chem. Commun.* **47**, 1878 (2011).
- [18] M.R. Delgado, R. Bulanek, P. Chlubna, and C.O. Areal, *Catal. Today* **252**, 214 (2015).
- [19] C.O. Areal, M.R. Delgado, P. Nachtigall, H.V. Thang, M. Rubes, R. Bulanek, and P. Chlubna-Eliasova. *Phys. Chem. Chem. Phys.* **16**, 10129 (2014).
- [20] C.O. Areal, O.V. Manoilova, G.T. Palomino, M.R. Delgado, A. A. Tsyganenko, B. Bonelli, and E. Garrone. *Phys. Chem. Chem. Phys.* **4**, 5713 (2002).
- [21] E. Garrone, and C.O. Areal. *Chem. Soc. Rev.* **34** (10), 846 (2005).
- [22] G.C. Bond, M.A. Keane, H. Kral, and J.A. Lercher, *Catal. Rev. Sci. Eng.* **42**, 223 (2000).
- [23] A.A. Tsyganenko, P.Yu. Storozhev, and C.O. Areal, *Kinet. Catal.* **45** (4), 530 (2004).
- [24] P. Nachtigall, O. Bludský, L. Grajciar, D. Nachtigallová, M. Rodríguez Delgado, and C. Otero Areal. *Phys. Chem. Chem. Phys.* **11** (5), 791 (2009).
- [25] M.R. Delgado, and C.O. Areal. *Energy* **36** (8) 5286 (2011).
- [26] C.O. Areal, *J. Mol. Struct.* **880**, 31 (2008).
- [27] C.O. Areal, O.V. Manoilova, A.A. Tsyganenko, G.T. Palomino, M.P. Mentrui, F. Geobaldo, and E. Garrone. *Eur. J. Inorg. Chem.* 1739 (2001).
- [28] M.R. Delgado, R. Bulanek, P. Chlubna, and C.O. Areal. *Catal. Today* **227**, 45 (2014).